Interaction of the Adenovirus Proteinase with Protein Cofactors with High Negative Charge Densities†

Neil S. Bajpayee, William J. McGrath, and Walter F. Mangel*

Biology Department, Brookhaven National Laboratory, Upton, New York 11973

Received February 7, 2005; Revised Manuscript Received March 21, 2005

ABSTRACT: The interactions of the human adenovirus proteinase (AVP) with polymers with high negative charge densities were characterized. AVP utilizes two viral cofactors for maximal enzyme activity (k_{cat}/K_m), the 11-amino acid peptide from the C-terminus of virion precursor protein pVI (pVIc) and the viral DNA. The viral DNA stimulates covalent AVP−pVIc complexes (AVP−pVIc) as a polyanion with a high negative charge density. Here, the interactions of AVP−pVIc with different polymers with high negative charge densities, polymers of glutamic acid (polyE), were characterized. The rate of substrate hydrolysis by AVP−pVIc increased with increasing concentrations of polyE. At higher concentrations of polyE, the increase in the rate of substrate hydrolysis approached saturation. Although glutamic acid did not stimulate enzyme activity, glutamic acid and NaCl could displace DNA from AVP−pVIc·(DNA) complexes; the K_i values were 230 and 329 nM, respectively. PolyE binds to the DNA binding site on AVP−pVIc as polyE and DNA compete for binding to AVP−pVIc. The equilibrium dissociation constant for 1.3 kDa polyE binding to AVP−pVIc was 56 nM. On average, one molecule of AVP−pVIc binds to 12 residues in polyE. Comparison of polyE and 12-mer single-stranded DNA interacting with AVP−pVIc revealed the binding constants are similar, as are the Michaelis−Menten constants for substrate hydrolysis. The number of ion pairs formed upon the binding of 1.3 kDa polyE to AVP−pVIc was 2, and the nonelectrostatic change in free energy upon binding was −6.5 kcal. These observations may be physiologically relevant as they infer that AVP may bind to proteins that have regions of negative charge density. This would restrict activation of the enzyme to the locus of the cofactor within the cell.

Human adenovirus serotype 2 (Ad2)[1] encodes a gene for a proteinase whose activity is absolutely essential for the synthesis of infectious virus (*1*). Late in infection, during virion assembly, ∼70 molecules (*2*) of the adenovirus proteinase (AVP) cleave multiple copies of six major virion precursor proteins at 3200 sites to render a virus particle infectious (*3*, *4*).

AVP is synthesized in an inactive form that requires cofactors for activation. One cofactor is pVIc, the 11-amino acid residue peptide from the C-terminus of adenovirus precursor protein pVI (*5*−*7*). A second cofactor is the viral DNA (*5*, *8*, *9*). These two cofactors stimulate the rate of substrate hydrolysis by AVP (*5*, *7*, *10*). Other proteinases bind to DNA (*11*), but only the enzymatic activity of AVP is stimulated by being bound to DNA. The crystal structure of the AVP−pVIc complex (AVP−pVIc), in which Cys10′ of pVIc forms a disulfide bond with Cys104 of AVP, is known (*12*, *13*), as are low-resolution models of AVP·(12-mer ssDNA) and AVP−pVIc·(12-mer ssDNA) complexes obtained by synchrotron X-ray footprinting (*9*).

The interaction of AVP with Ad2 DNA as a cofactor is not dependent upon a specific nucleic acid sequence. T7 DNA substituted for Ad2 DNA, as did single-stranded DNAs, circular single- and double-stranded DNAs, and even transfer RNAs. Rather, it appeared as if the requirement was for a polymer with a high negative charge density. Polyglutamic acid (polyE), polyaspartic acid, and heparin substitute for Ad2 DNA but not the four deoxyribonucleoside monophosphates, glutamic acid, aspartic acid, or polylysine. The major polyanion with a high negative charge density in the virus particle is, of course, the viral DNA. A model has been presented suggesting that in the virion AVP moves along the viral DNA looking for precursor protein cleavage sites much as RNA polymerase moves along DNA looking for a promoter (*8*).

AVP contains two domains (*12*, *13*), and both pVIc and DNA (*9*) appear to bind to AVP as straps holding the two domains of AVP together. Both cofactors bind with physiologically relevant equilibrium dissociation constants, K_d. The K_d for the binding of pVIc to AVP is 4.4 μM (*7*) and for the binding of 12-mer dsDNA to AVP 64 nM (*8*). The K_d for the binding of 12-mer dsDNA to AVP−pVIc complexes is

† Research supported by the Office of Biological and Environmental Research of the U.S. Department of Energy under Prime Contract DE-AC0298CH10886 with Brookhaven National Laboratory, and by National Institutes Health Grant AI41599. N.S.B. was supported by the Department of Energy's Office of Science Education and Technical Information by a Student Undergraduate Laboratory Internship.

* To whom correspondence should be addressed. Telephone: (631) 344-3373. Fax: (631) 344-3407. E-mail: Mangel@bnl.gov.

[1] Abbreviations: Ad2, human adenovirus serotype 2; AVP, recombinant adenovirus proteinase; AVP−pVIc, 1:1 covalent complex of AVP with pVIc; AVP−pVIc·(polyE), noncovalent complex between AVP−pVIc and polyE; dsDNA, double-stranded DNA; IHF, integration host factor; K_a, equilibrium association constant; k_{cat}, catalytic rate constant for substrate hydrolysis; K_d, equilibrium dissociation constant; K_m, Michaelis constant; polyE, polyglutamic acid; pVI, precursor to virion protein VI; pVIc, 11-amino acid peptide (GVQSLKRRRCF) from the C-terminus of pVI; ssDNA, single-stranded DNA.

10.1021/bi0502240 CCC: $30.25
Published on Web 05/26/2005

4.6 nM. The crystal structure of AVP−pVIc (*12*, *13*) indicates that pVIc binds quite far from the active site of AVP. The distance between Cys10′ of pVIc and Cys122, the active site nucleophile, is more than 30 Å (*12*, *13*). A low-resolution model of the DNA binding site on AVP−pVIc obtained by synchrotron protein footprinting indicates that part of the DNA binding site overlaps with the pVIc binding site (*9*).

Here we characterize the interaction of AVP−pVIc with polymers of glutamic acid and compare that interaction to the interaction of AVP−pVIc with DNA (*8*). PolyE is a cofactor for the adenovirus proteinase, because enzyme activity was stimulated by polyE. AVP−pVIc complexes bound 1.3 kDa polyE with a K_d of 56 nM. When polyE binds to AVP−pVIc, the k_{cat} for substrate hydrolysis increased significantly. In comparison, the binding of 12-mer ssDNA to AVP−pVIc complexes exhibited a K_d of 109 nM. The k_{cat} for substrate hydrolysis also increased significantly upon the binding of 12-mer ssDNA to AVP−pVIc complexes. These results may be physiologically relevant as there is an AVP binding site on actin that has the same characteristic described here for polyE (W. F. Mangel and M. T. Brown, unpublished observations).

EXPERIMENTAL PROCEDURES

Materials. pVIc (GVQSLKRRRCF) and the 5′-fluorescein-labeled 12-mer ssDNA (GACGACTAGGAT) were purchased from Research Genetics (Huntsville, AL). Ellman's reagent, 5,5′-dithiobis(2-nitrobenzoate) or DTNB; Ad2 DNA; glutamic acid; and glutamic acid polymers with molecular masses of 10.6, 18.1, 51.3, and 66 kDa were purchased from Sigma Chemical Co. (St. Louis, MO). The 1.3 kDa glutamic acid polymer 10-mer was purchased from New England Peptide, Inc. (Gardner, MA). Octyl glucoside was purchased from Fisher Scientific (Faden, NJ). The fluorogenic substrate $(Leu\text{-}Arg\text{-}Gly\text{-}Gly\text{-}NH)_2$-rhodamine was synthesized and purified as described previously (*5*, *10*). AVP was expressed in *Escherichia coli* and purified as described previously (*5*, *14*).

Protein Concentration. Protein concentrations were determined using the BCA protein assay from Pierce Chemical Co. (Rockford, IL). For the concentration of AVP, a calculated molar absorbance coefficient at 280 nm of 26 510 was used (*15*). The concentration of pVIc was determined by titration of its cysteine residue with Ellman's reagent. A molar extinction coefficient at 412 nm of 14 150 was used to calculate the concentration of thionitrobenzoate (*16*).

Formation of Covalent AVP−pVIc Complexes. Covalent complexes between AVP and pVIc, held together by a disulfide bond between Cys104 of AVP and Cys10′ of pVIc, were prepared by incubating at 4 °C equal molar concentrations (50 μM) of AVP and pVIc in 5 mM Tris (pH 8.0), 5 mM NaCl, and 0.1 mM EDTA.

Proteinase Activity Assays. Enzyme activity assays contained, in 1 mL, 10 mM Tris-HCl (pH 8.0), 2 mM octyl glucoside, AVP−pVIc, and in some cases polymers of glutamic acid or 12-mer ssDNA. Assay mixtures were preincubated for 5 min at 37 °C prior to the addition of the fluorogenic substrate $(Leu\text{-}Arg\text{-}Gly\text{-}Gly\text{-}NH)_2$-rhodamine. The increase in fluorescence at 37 °C was monitored as a function of time in an ISS (Urbana, IL) PC-1 spectrofluorometer. The excitation wavelength was 492 nm and the emission wavelength 523 nm, both set with a band-pass of 8 nm. Assays for measuring the K_m and k_{cat} values in the presence of polymers of glutamic acid were performed with polyE concentrations at least 5-fold greater than the K_d. The concentration of the fluorogenic substrate was varied from 0.2 to 5 times the K_m.

Fluorescence Anisotropy Experiments To Determine the K_d for the Binding 12-mer ssDNA to AVP−pVIc. Fluorescence anisotropy experiments were performed at 25 °C in the thermostated sample compartment of an ISS PC-1 spectrofluorometer. An Oriel 530 nm band-pass filter was inserted before the emission photomultiplier. The excitation wavelength was 490 nm. The excitation slit width was 8 nm.

The K_d for the binding of 12-mer ssDNA to AVP−pVIc was obtained by measuring the anisotropy of 1 nM fluorescein-labeled 12-mer ssDNA in 10 mM Tris-HCl (pH 8.0) and 2 mM octyl glucoside. Then, an aliquot of AVP−pVIc was added. After binding equilibrium had been reached, usually within 90 s, the change in anisotropy was measured for 30 s. A second aliquot was added and the process repeated until no further change in anisotropy was observed.

The K_d was calculated from the fluorescence anisotropy data as follows. The anisotropy, r, is defined as

$$r = (I_{||} - GI_{\perp})(I_{||} + 2GI_{\perp})^{-1}$$

where $I_{||}$ and $I_{\perp}$ are the fluorescence emission intensities with polarizers parallel and perpendicular, respectively, to that of the exciting beam. The instrument correction factor G was determined for each experiment by measuring the $I_{\perp}/I_{||}$ ratio from horizontally polarized light. The fraction of ligand bound, f_b, at any ligand concentration is

$$f_b = (r_{obs} - r_o)/(r_{max} - r_o) \text{ and } f_f = 1 - f_b$$

where r_o is the initial anisotropy of the DNA in the absence of other components, r_{obs} is the anisotropy at the specific ligand concentration, r_{max} is the anisotropy when the enzyme is saturated with ligand, and f_f is the fraction of ligand free. The concentrations of free ligand, L_f, and bound ligand, L_b, are

$$L_f = f_f[\text{DNA}] \text{ and } L_b = f_b[\text{DNA}]$$

where [DNA] is the molar concentration of DNA molecules. From a plot of L_b versus L_f, the K_d can be obtained as the concentration of L_f at which L_b is 50% maximal L_b; the K_d obtained this way is valid only if the stoichiometry of binding of the ligand to AVP is 1:1.

Fluorescence Anisotropy Experiments To Determine the K_d for the Binding of 1.3 kDa PolyE to AVP−pVIc. The K_d for the binding of 1.3 kDa polyE to AVP−pVIc was determined by measuring the displacement of 12-mer ssDNA from AVP−pVIc·(12-mer ssDNA) complexes by increasing concentrations of 1.3 kDa polyE. These experiments were carried out at 25 and 37 °C. AVP−pVIc at a concentration 5-fold greater than the K_d for 12-mer ssDNA and 1 nM 5′-fluorescein-labeled 12-mer ssDNA were incubated in 10 mM Tris-HCl (pH 8.0) and 2 mM octyl glucoside for 90 s. In experiments carried out at 25 °C, the AVP−pVIc concentration was 49 nM, 40 nM for those done at 37 °C. The anisotropy was measured for 30 s. Then, an aliquot of polyE

was added. After 90 s, the anisotropy was measured. This process was repeated until no further decrease in anisotropy was observed. The K_d was calculated as described by Kuzmic et al. (*17*).

Nonelectrostatic Free Energy of Binding of AVP−pVIc to 1.3 kDa PolyE. Fluorescence anisotropy was also used to determine the equilibrium association constants, K_a, for binding of AVP−pVIc to 1.3 kDa polyE as a function of the NaCl concentration. Binding assays were carried out at 25 °C in solutions initially containing 1.8 mL of 10 mM Tris-HCl (pH 8.0), 2 mM octyl glucoside, 1 nM 5′-fluorescein-labeled 12-mer ssDNA, and either 0, 1, 2, 3, or 4 mM NaCl. The anisotropy of the solutions in the absence of ligand was determined at each NaCl concentration. Then, AVP−pVIc complexes were added, and after binding equilibrium had been reached, usually 2 min, the change in anisotropy was measured. This process was repeated until saturation curves were obtained. At each concentration of NaCl, the concentration of AVP−pVIc varied from 0.2 to at least 3 times the calculated K_a. At higher concentrations of NaCl, the AVP−pVIc concentration varied from 0.2 to 2 times the calculated K_a. Then, an aliquot of 1.3 kDa polyE was added. After 90 s, the anisotropy was measured, and the process was repeated until no further decrease in anisotropy was observed.

The K_a was calculated as described above for calculation of the K_d (*17*), where $K_a = 1/K_d$.

Stoichiometry of Binding of AVP−pVIc to Glutamic Acid Polymers with Molecular Masses of 1.3, 10.6, 18.1, 51.3, and 66 kDa. The number of AVP−pVIc binding sites per glutamic acid polymer was measured by activity assays under tight binding conditions, i.e., under conditions where the concentration of AVP−pVIc was at least 3-fold greater than the apparent K_d. Increasing concentrations of polyE were added to a constant concentration of AVP−pVIc, and the rates of substrate hydrolysis were measured.

Lifetime of the Excited State. The lifetime of the excited state of a fluorescein moiety attached to DNA was measured in an SLM 4800 spectrofluorometer using an excitation wavelength of 490 nm and an Oriel 520 nm band-pass filter before the emission photomultiplier. The phase shift method with a frequency modulator tank filled with 19% ethanol to generate sinusoidally varying excitation light was used (*18*). All measurements were taken at a setting of 18 MHz in solutions of 25 mM Hepes (pH 8.0) containing 12.5 nM 18-mer dsDNA labeled at one of its 5′ ends with fluorescein in the absence or presence of 235 nM AVP−pVIc.

RESULTS

PolyE Acts as a Cofactor for AVP−pVIc. PolyE is a cofactor, because it stimulates the rate of substrate hydrolysis by AVP−pVIc. Increasing concentrations of 10.6 kDa polyE were incubated with a constant amount of AVP−pVIc, and after 5 min at 37 °C, the fluorogenic substrate (Leu-Arg-Gly-Gly-NH)$_2$-rhodamine was added. The increase in fluorescence, from the product of the reaction, (Leu-Arg-Gly-Gly-NH)-rhodamine, was measured as a function of time. The results are shown in Figure 1. For each concentration of polyE, the increase in fluorescence with time was linear. The rate of substrate hydrolysis increased with increasing polyE concentrations. At higher polyE concentrations, the rate of substrate hydrolysis approached a plateau, implying that the enzyme complex could be saturated with polyE. Thus, polyE can indeed act as a cofactor for AVP−pVIc. As a control experiment, under the same experimental conditions, with concentrations of glutamic acid equivalent to the total concentration of glutamic acid residues at the various concentrations of polyE used in the experiments in Figure 1, no stimulation of AVP−pVIc activity was observed (data not shown).

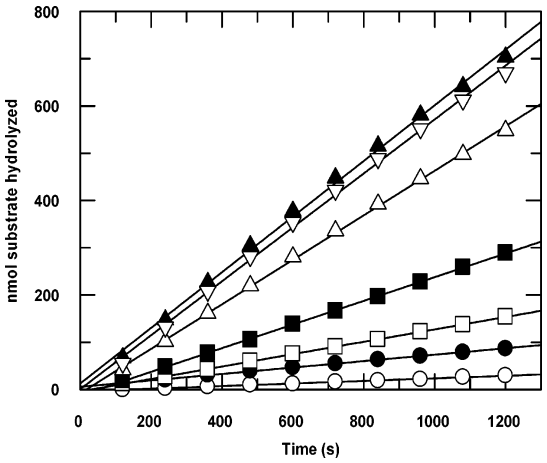

FIGURE 1: Stimulation of AVP−pVIc by polyE. Increasing concentrations of 10.6 kDa polyE at 0 (○), 2 (●), 4 (□), 8 (■), 20 (△), 40 (▽), and 50 nM (▲) were incubated with 150 nM AVP−pVIc for 5 min at 37 °C, after which 15 μM (Leu-Arg-Gly-Gly-NH)$_2$-rhodamine was added, and the increase in fluorescence (nmol substrate hydrolyzed) was measured as a function of time.

PolyE Binds to the DNA Binding Sites on AVP−pVIc. Since polyE is a polymer with a high negative charge density as is the viral DNA, it may bind to the same sites on AVP−pVIc. To test this hypothesis, we set up a competition between polyE and DNA. Increasing concentrations of AVP−pVIc were added to 1 nM 12-mer ssDNA that had fluorescein attached to its 5′ end. Binding was monitored by changes in fluorescence anisotropy. The results (Figure 2A) showed that the change in fluorescence anisotropy increased with increasing concentrations of AVP−pVIc until a plateau was reached. At the plateau, increasing concentrations of 1.3 kDa polyE were then added (Figure 2B). As the concentrations of 1.3 kDa polyE were increased, the change in fluorescence anisotropy decreased until all the 12-mer ssDNA was displaced. Thus, polyE and DNA appeared to be binding to the same sites on AVP−pVIc.

Equilibrium Dissociation Constant for the Binding of 1.3 kDa PolyE to AVP−pVIc. The K_d for the binding of 1.3 kDa polyE to AVP−pVIc was calculated as described in Experimental Procedures using the data in Figure 2B. The apparent K_d for the binding of AVP−pVIc to 1.3 kDa polyE at 25 °C was 56 nM (Table 1). The K_d is apparent, because the calculation used to obtain the K_d assumed the stoichiometry of binding of AVP−pVIc to 1.3 kDa polyE was 1:1. When this experiment was performed at 37 °C, the apparent K_d was 50 nM (data not shown). The data in Figure 2A were used to calculate the K_d for the binding of 12-mer ssDNA to AVP−pVIc (Table 1).

Stoichiometry of Binding of AVP−pVIc to 1.3 kDa PolyE. Enzyme activity assays under tight binding conditions were used to ascertain the stoichiometry of binding of AVP−pVIc to 1.3 kDa polyE. AVP−pVIc complexes were incubated at

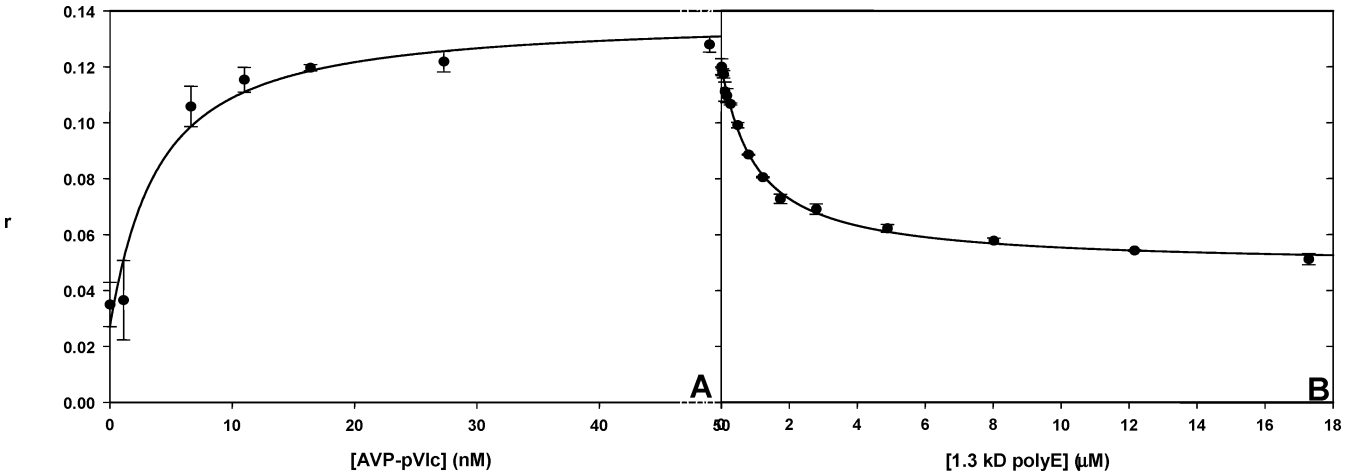

FIGURE 2: Equilibrium dissociation constant for the binding of 12-mer ssDNA to AVP−pVIc (A) and for the binding of 1.3 kDa polyE to AVP−pVIc (B). (A) The anisotropy (*r*) of a 1.8 mL solution of 1 nM 12-mer ssDNA with fluorescein attached to the 5′ end was measured at 25 °C. Then, an aliquot of AVP−pVIc was added and, after 90 s, the anisotropy measured. This was repeated until there was no further increase in anisotropy. (B) Next, an aliquot of 1.3 kDa polyE was added and, after 90 s, the anisotropy measured. This was repeated until no further decrease in anisotropy was observed. The equilibrium dissociation constant from the data in panel A was calculated as described in Experimental Procedures. The equilibrium dissociation constant from the data in panel B was calculated using the method of Kuzmic et al. (*17*).

Table 1: Interactions of AVP−pVIc with Polyanions

Equilibrium Dissociation Constants (K_d) for the Binding of AVP−pVIc to PolyE and DNA[a]	
1.3 kDa polyE	
25 °C	56 ± 6 nM
37 °C	50 ± 8 nM
12-mer ssDNA	
25 °C	13 ± 4 nM
37 °C	7 ± 1 nM
Michaelis−Menten Constants for AVP−pVIc with or without PolyE or DNA[b]	
1.3 kDa polyE	
K_m	7 ± 1 μM
k_{cat}	2 ± 0.2 s^{-1}
18.1 kDa polyE	
K_m	0.033 ± 0.012 μM
k_{cat}	2.7 ± 0.2 s^{-1}
12-mer ssDNA	
K_m	3 ± 1 μM
k_{cat}	3 ± 0.3 s^{-1}
no polyE or DNA	
K_m	5 ± 2 μM
k_{cat}	0.36 ± 0.04 s^{-1}

Displacement of DNA from AVP−pVIc·(DNA) Complexes[c]

	K_i (nM)
glutamic acid	230 ± 23
NaCl	329 ± 50

[a] Equilibrium dissociation constants (K_d) for the binding of fluorescein-labeled 12-mer ssDNA to AVP−pVIc and its displacement by 1.3 kDa polyE, at two temperatures, as determined by fluorescence anisotropy. [b] Michaelis−Menten constants determined with two polymers of glutamic acid and AVP−pVIc using the fluorogenic substrate (Leu-Arg-Gly-Gly-NH)$_2$-rhodamine. [c] The K_i is the concentration of glutamic acid or NaCl required to displace half of the 12-mer ssDNA bound to AVP−pVIc, as determined by fluorescence anisotropy.

37 °C with increasing concentrations of 1.3 kDa polyE, and the rate of substrate hydrolysis was measured. The concentration of AVP−pVIc was 150 nM, 3-fold greater than the apparent K_d. As the concentration of 1.3 kDa polyE was increased, below the concentration of 1.3 kDa polyE binding sites on AVP−pVIc, no free 1.3 kDa polyE was present; thus, the rate of substrate hydrolysis was directly proportional to the concentration of 1.3 kDa polyE (Figure 3A). When the concentration of 1.3 kDa polyE exceeded that of the 1.3 kDa polyE binding sites on AVP−pVIc, no further increase in the rate of substrate hydrolysis was observed. The data were characterized by two straight lines whose intersection reflected the minimal concentration of 1.3 kDa polyE required to saturate AVP−pVIc. Extrapolation of the intersection point to the abscissa indicated that 150 nM 1.3 kDa polyE saturated 150 nM AVP−pVIc. Therefore, the stoichiometry of binding was 1:1, and the K_d, as opposed to the apparent K_d, at 25 °C was 56 ± 6 nM.

Stoichiometry of Binding of AVP−pVIc to Polymers of Glutamic Acid of Different Lengths. The stoichiometries of binding of AVP−pVIc to polymers of glutamic acid with average molecular masses of 10.6, 18.1, 51.3, and 66 kDa were determined as described for determination of the stoichiometry of binding of AVP−pVIc to 1.3 kDa polyE. An example of the data that were obtained, with 66 kDa polyE, is shown in Figure 3B. Extrapolation of the intersection points to the abscissa indicated that 2.6 nM 66 kDa polyE saturated 100 nM AVP−pVIc. Therefore, the stoichiometry of binding was 38:1 AVP−pVIc:66 kDa polyE. The stoichiometries of binding of five polymers of glutamic acid to AVP−pVIc are listed in Table 2; the stoichiometries of binding (AVP−pVIc:polyE) were 1:1, 6:1, 15:1, 34:1, and 38:1 for 1.3, 10.6, 18.1, 51.3, and 66 kDa polyE, respectively. The stoichiometry of binding increased linearly with increasing lengths of the glutamic acid polymers. By dividing the average number of glutamic acid residues in each polymer by the maximal number of AVP−pVIc complexes bound per polymer, we can calculate the number of glutamic acid residues per enzyme (Table 2). The average is 12 ± 2. This average was calculated without using the data from the 1.3 kDa polymer of glutamic acid, because, as mentioned in the Discussion, it may not contain a complete polyE binding site.

Comparison of the Cofactor Activity of PolyE to That of Viral DNA. The macroscopic kinetic constants, K_m and k_{cat}, for the hydrolysis of (Leu-Arg-Gly-Gly-NH)$_2$-rhodamine by

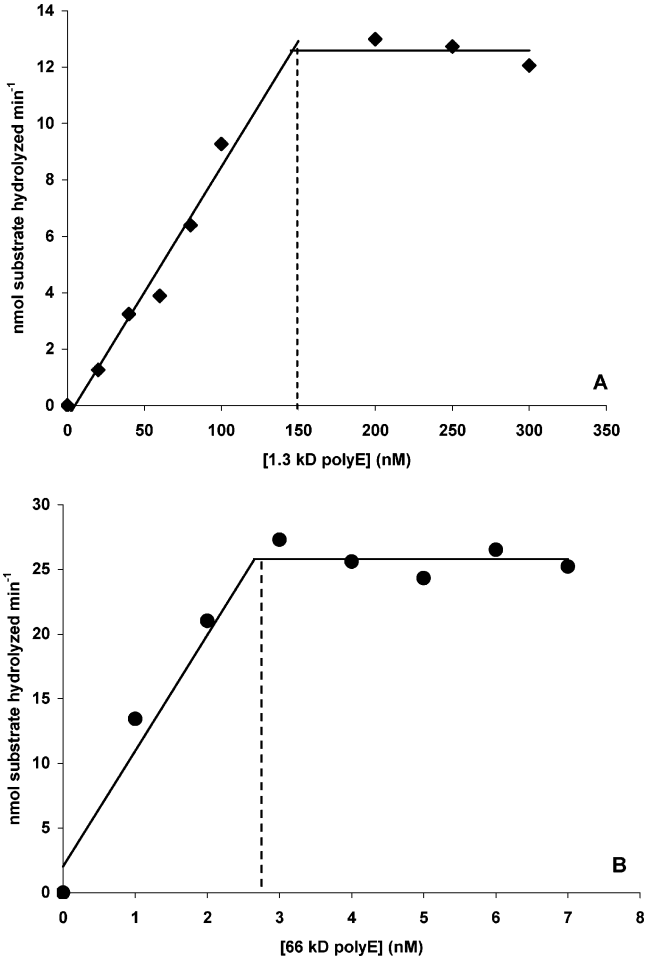

FIGURE 3: Stoichiometry of binding of AVP−pVIc to 1.3 kDa polyE (A) and 66 kDa polyE (B). Increasing concentrations of polyE were incubated with (A) 150 nM AVP−pVIc or (B) 100 nM AVP−pVIc. After 5 min at 37 °C, (Leu-Arg-Gly-Gly-NH)$_2$-rhodamine was added and the rate of substrate hydrolysis measured. The solid lines were drawn with a least-squares regression analysis. The dashed lines were drawn from the intersection of the solid lines to the abscissa.

complexes of AVP−pVIc with 18.1 kDa polyE, were determined at 37 °C by incubating 10 nM AVP−pVIc with 1 nM 18.1 kDa polyE. After 5 min, different concentrations of (Leu-Arg-Gly-Gly-NH)$_2$-rhodamine were added and the rate of substrate hydrolysis was measured (Figure 4). The K_m and k_{cat} values were 33 ± 12 nM and 2.7 ± 0.2 s^{-1}, respectively (Table 1). In a similar experiment, but with 1.3 kDa polyE, the K_m was 7 ± 1 μM and the k_{cat} was 2 ± 0.1 s^{-1}. In comparison, the macroscopic kinetic constants, K_m and k_{cat}, for the hydrolysis of (Leu-Arg-Gly-Gly-NH)$_2$-rhodamine by complexes of AVP−pVIc were 5 ± 2 μM and 0.36 ± 0.04 s^{-1}, respectively. In the presence of adenovirus DNA, the K_m is 3 ± 1 μM and the k_{cat} is 3 ± 0.3 s^{-1} (*8*).

Number of Ion Pairs Formed upon the Binding of AVP−pVIc to 1.3 kDa PolyE. The number of ion pairs involved in binding of AVP−pVIc to 1.3 kDa polyE was obtained from equilibrium association constants (K_a) determined at different ionic strengths. The K_a values were obtained in competition experiments between polyE and DNA. Increasing concentrations of AVP−pVIc were added to 1 nM 12-mer ssDNA that had fluorescein attached to its 5′ end. Binding was monitored by changes in fluorescence anisotropy. Once saturation was reached, where no further increase in anisotropy was observed upon the addition of more AVP−pVIc, increasing concentrations of 1.3 kDa polyE were then added. As the concentrations of 1.3 kDa polyE were increased, the change in fluorescence anisotropy decreased until all the 12-mer ssDNA was displaced. From these data (data not shown), a K_a could be calculated (*17*). The K_a values at 1, 2, 3, and 4 mM NaCl were 8.3 × 10^6, 6.0 × 10^6, 3.5 × 10^6, and 2.5 × 10^6 M, respectively. The log K_a was plotted versus −log[NaCl] (Figure 5). The following equation (*19*) describes the resultant straight line:

$$-\frac{\partial \log K_a}{\partial \log[Na^+]} = m'\psi$$

where [Na$^+$] is the monovalent counterion concentration, m' is the number of ion pairs formed, and ψ is the fraction of a counterion associated, in the thermodynamic sense, with each side chain of a polymer of glutamic acid in solution. The polyanion poly-L-glutamic acid is modeled as a cylindrical rod with a length per unit charge equal to 0.35 nm (*20*). This distance is much shorter than the Bjerrum length of 0.71 nm for polyelectrolytes containing monovalent charge groups. Therefore, the dimensionless linear charge density, ξ, defined as the ratio of Bjerrum length to length per unit charge is 2.0; a ratio greater than 1.0 implies a certain fraction of the charge on the polyanion is neutralized due to direct condensation of counterions such as Na$^+$. The fraction of counterion associated thermodynamically is determined by $\psi = 1 - \xi^{-1}$, and for polyE, it is equal to 0.51. Thus, the number of ion pairs formed, m', was 1.7.

Nonelectrostatic Change in Free Energy upon the Binding of AVP−pVIc to 1.3 kDa PolyE. The nonelectrostatic change in free energy, ΔG_0^0, upon binding of AVP−pVIc to 1.3 kDa polyE was also calculated. The line in Figure 5 was extrapolated to a Na$^+$ concentration of 1 M, yielding a K_a in 1 M NaCl of 46 μM. Then, the following equation was used:

$$\Delta G_0^0 = -RT \ln K_o$$

where K_o is K_a in 1 M Na$^+$. The ΔG_0^0 (1 M Na$^+$) was −6.15 kcal. By correcting for two lysine-like ion pairs, which have a ΔG_{lys}^0 (1 M Na$^+$) of 0.18 kcal, we calculated a nonelectrostatic free energy of binding of −6.5 kcal.

DISCUSSION

The data presented here clearly showed that polyE is a cofactor for the adenovirus proteinase. Enzyme activity was stimulated by polyE. AVP−pVIc complexes bound to 1.3 kDa polyE with a K_d of 56 nM. When polyE bound to AVP−pVIc, the k_{cat} for substrate hydrolysis increased significantly. In comparison, the binding of 12-mer ssDNA to AVP−pVIc complexes exhibited a K_d of 13 nM. The k_{cat} for substrate hydrolysis also increased significantly upon the binding of 12-mer ssDNA to AVP−pVIc complexes.

The K_d values for binding of polyE or DNA to AVP−pVIc were obtained in competition experiments in which the binding of polyE, spectrofluorometrically invisible, was observed because of its ability to displace fluorescein-labeled DNA from an AVP−pVIc·(fluorescein-labeled DNA) complex. The mathematical treatment of the data (*17*) took into

Table 2: Stoichiometries of Binding of AVP−pVIc to Polymers of Glutamic Acid of Different Lengths

	1.3 kDa polyE	10.6 kDa polyE	18.1 kDa polyE	51.3 kDa polyE	66 kDa polyE
AVP:polyE stoichiometry[a]	1:1	6:1	15:1	34:1	38:1
no. of Glu residues bound[b] per AVP	10	14	9	12	13

[a] Number of AVP−pVIc molecules binding per polyE molecule. [b] Number of glutamic acid residues in polyE bound by one AVP−pVIc molecule.

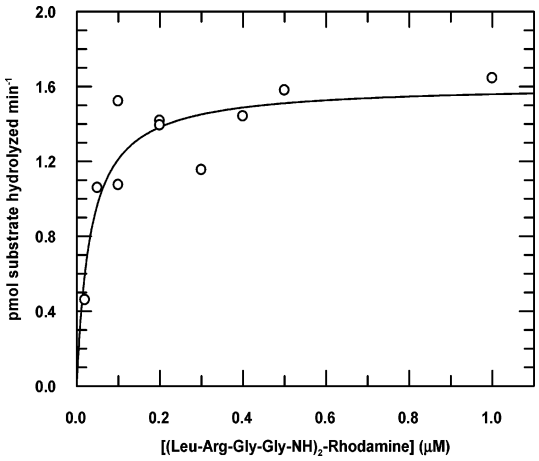

FIGURE 4: Macroscopic kinetic constants for the hydrolysis of (Leu-Arg-Gly-Gly-NH)$_2$-rhodamine by AVP−pVIc•(polyE) complexes. Reaction mixtures containing 10 nM AVP−pVIc and 1 nM 18.1 kDa polyE were incubated for 5 min at 37 °C. Then, (Leu-Arg-Gly-Gly-NH)$_2$-rhodamine, at concentrations ranging from 0.02 to 1 μM, was added and the increase in fluorescence with time measured. The K_m was 33 ± 12 nM, and the k_{cat} was 2.7 ± 0.2 s^{-1}.

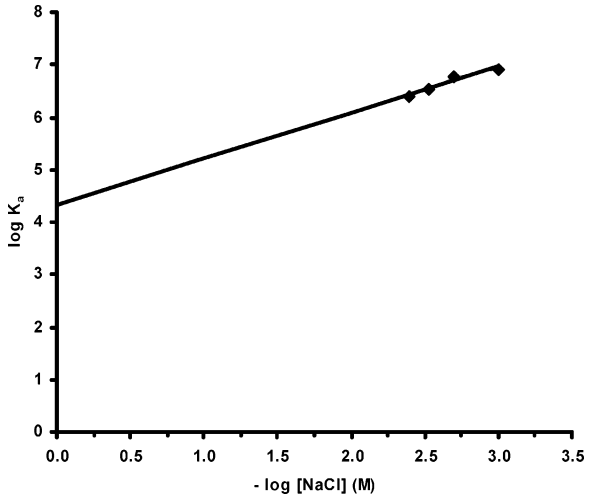

FIGURE 5: Number of ion pairs formed upon the binding of AVP−pVIc to 1.3 kDa polyE and the nonelectrostatic change in free energy upon the binding of AVP−pVIc to 1.3 kDa polyE. Equilibrium dissociation constants for the binding of 1.3 kDa polyE to AVP−pVIc in 1, 2, 3, and 4 mM NaCl were measured as follows. The anisotropy (r) of a 1.8 mL solution of 1 nM 12-mer ssDNA with fluorescein attached to the 5′ end was measured at 25 °C. Then, an aliquot of AVP−pVIc was added and, after 90 s, the anisotropy measured. This was repeated until there was no further increase in anisotropy. Next, an aliquot of 1.3 kDa polyE was added and, after 90 s, the anisotropy measured. This was repeated until no further decrease in anisotropy was observed. The equilibrium dissociation constants were calculated from these data using the method of Kuzmic et al. (*17*). The K_d values for binding of 1.3 kDa polyE to AVP−pVIc in 1, 2, 3, and 4 mM NaCl were 121, 167, 287, and 406 nM, respectively.

account the multiple equilibria that were present. The equilibrium equation for mixtures of two mutually competitive tight binding ligands was expressed in a recursive form in which the dependent variable appears on both sides of the equation, and the solution was found iteratively. The method of analysis used to calculate K_d assumed the stoichiometry of binding of AVP−pVIc to 1.3 kDa polyE was 1:1. And this was shown to be the case. The minimum concentration of 1.3 kDa polyE required to saturate 150 nM AVP−pVIc was 150 nM. A similar stoichiometry of binding was exhibited upon the binding of AVP−pVIc to 12-mer ssDNA (*8*).

The K_d values are relatively low. The K_d for the binding of AVP−pVIc to 12-mer ssDNA was 13 nM, the forward reaction in Figure 2A. This compares favorably with a K_d of 18 nM obtained by enzyme activity assays (*8*). In the reverse reaction in Figure 2B, the K_d for the binding of AVP−pVIc to 1.3 kDa polyE was 56 nM. There was very little difference in K_d values if binding was carried out at 25 or 37 °C (Table 1). One reason the K_d for 1.3 kDa polyE is higher than that for 12-mer ssDNA is that the length of the 1.3 kDa polyE may not be optimal for binding. With the longer polymers of glutamic acid, one AVP−pVIc molecule bound to an average of 12 residues (Table 2). The 1.3 kDa polyE contains 10 glutamic acid residues. If the 1.3 kDa polyE were slightly longer, perhaps its K_d for AVP−pVIc would decrease.

There are several indications that the K_d values for the binding of AVP−pVIc to polyE are correct. None of the binding curves obtained by fluorescence anisotropy gave any indication of more than one type of binding reaction. This implied that binding of the enzyme was not occurring preferentially at the ends of the polyE molecules. Also, in the fluorescence anisotropy experiments, competition was observed between fluorescein-labeled 12-mer ssDNA and polyE for binding sites on AVP−pVIc. This implied that AVP−pVIc was not binding to the fluorescein moiety on DNA. Measurement of the stoichiometry of binding of AVP−pVIc to 1.3 or 66 kDa polyE required one of the components in the reactions be at least 3-fold higher than the K_d. This was shown to be correct. With 150 nM AVP−pVIc, tight binding was exhibited at 37 °C at low, 25−50 nM, concentrations of 1.3 kDa polyE, implying the K_d was much less than 150 nM. Measurement of the K_d for binding of AVP−pVIc to 1.3 kDa polyE yielded a K_d of 50 nM.

The results from the fluorescence anisotropy experiments clearly indicated that polyE was binding to the same sites on AVP−pVIc that DNA does, and thus like DNA, polyE was binding nonspecifically to AVP−pVIc. PolyE binds to the same sites on AVP−pVIc that DNA does, because polyE was able to displace completely fluorescein-labeled 12-mer ssDNA from AVP−pVIc; the anisotropy returned to its level in the absence of DNA. The binding of 12-mer ssDNA and polyE to AVP−pVIc can be completely abolished by NaCl. The equilibrium inhibitor constant, K_i, was 329 nM (Table 1). Although glutamic acid bound to AVP−pVIc(DNA) complexes with a K_i of 230 nM (similar to the K_i of NaCl),

it cannot stimulate enzyme activity. It is this type of observation that led to the conclusion that only polymers with high negative charge densities can stimulate AVP−pVIc (*5*). The results from the stoichiometry of binding experiments are consistent with the conclusion that polyE, like DNA, was binding nonspecifically to AVP−pVIc. Three AVP−pVIc molecules saturate the binding sites on one 18-mer dsDNA, and six AVP−pVIc molecules saturate the binding sites on one 36-mer dsDNA (*8*). On Ad2 DNA, there are ∼3027 binding sites. With polymers of glutamic acid, the stoichiometries of binding (AVP−pVIc:polyE) are 1:1, 6:1, 15:1, 34:1 and 38:1 with 1.3, 10.6, 18.1, 51.3, and 66 kDa polyE, respectively. Thus, on average, one molecule of AVP−pVIc binds to six nucleotides or 12 glutamic acid residues.

Binding of polyE or DNA to AVP−pVIc alters the interaction of the enzyme with the fluorogenic substrate (Leu-Arg-Gly-Gly-NH)$_2$-rhodamine. In the absence of these cofactors, the K_m was 5 μM and the k_{cat} 0.36 s^{-1}. Both the viral DNA and 1.3 kDa polyE increased the k_{cat} for substrate hydrolysis over that of AVP−pVIc by a factor of 6−7. Neither the viral DNA nor the 1.3 kDa polyE decreased the K_m. However, the 18.1 kDa polyE decreased the K_m by a factor of 150. Since the length of the 1.3 kDa polyE may not be optimal for binding and substrate hydrolysis, perhaps with slightly longer polymers of glutamic acid, the K_m would drop to the level of that exhibited by the 18.1 kDa polyE.

Several control experiments were performed to ensure that in the fluorescence anisotropy experiments the binding of ligand to DNA was indeed being measured. For the conclusions in the fluorescence anisotropy experiments to be valid, the lifetime of the excited state of the fluorophore must not change during the assay. The lifetime of the excited state of the fluorescein moiety attached to one of the 5′ ends of 18-mer dsDNA was 2.3 ± 0.4 ns, and it did not change by more than 10% when the DNA was saturated with ligand (data not shown). As a control, the lifetime of the excited state of free fluorescein was measured using 0.1% (w/v) magnesium oxide as a standard reference scattering solution. Free fluorescein consistently gave a lifetime of 3.7 ± 0.9 ns. Each lifetime measurement was the average of 10 readings. Another indication the ligands were binding to DNA was that changes in anisotropy were sensitive to the presence of NaCl. If DNA saturated with ligand was incubated in 200 mM NaCl, the anisotropy returned to its value in the absence of ligand. Last, the ligands that bound to DNA were not binding to the fluorescein moiety on DNA. When a constant amount of AVP−pVIc and fluorescein-labeled 18-mer dsDNA were incubated with increasing amounts of unlabeled 18-mer dsDNA, the change in anisotropy decreased in proportion to the amount of unlabeled 18-mer dsDNA added (data not shown). This signified competition between fluorescein-labeled 18-mer dsDNA and unlabeled 18-mer dsDNA for binding sites on AVP−pVIc and implied that AVP−pVIc was not binding to the fluorescein moiety on DNA.

The non-sequence specific interaction between AVP−pVIc and polyE exhibited a substantial dependence on monovalent sodium ion concentration (Figure 5). This dependence reflects the electrostatic component of the binding reaction (*19*). The electrostatic component originates from the formation of ion pairs between positively charged groups on AVP−pVIc and negatively charged carboxyl groups on polyE. Upon binding, there may be a concomitant release of counterions from the polyE and, possibly, from AVP−pVIc. From an analysis of the equilibrium association constants for the binding of AVP−pVIc to 1.3 kDa polyE as a function of the Na^+ concentration, an accurate estimate of the number of ion pairs involved in the interaction was obtained. Two ion pairs were involved in complex formation with AVP−pVIc and 1.3 kDa polyE. For comparison, two ion pairs are involved in complex formation with 12-mer dsDNA and AVP−pVIc (*8*); with the T4 gene 32 protein, two ion pairs are involved in non-sequence specific binding to helical DNA (*19*).

A different interpretation of the data for the binding of polyE to AVP−pVIc as a function of ionic strength is that the salt concentration dependences we observed are the result of "coupled salt bridge disruptions". In a calorimetric study of binding of integration host factor (IHF) to a 34 bp DNA oligomer containing the H′ site of λ phage, very negative and highly salt concentration dependent binding enthalpies were observed (*21*). These could not be explained in terms of DNA deformation (*22*) but could be understood in terms of the hydration of IHF carboxylates upon DNA binding (*21*). In the absence of DNA, cationic residues on IHF form dehydrated surface salt bridges (∼3 Å charge separation) to neighboring carboxylates. In the presence of DNA, these cationic residues on the protein change partners by interacting with the DNA phosphates. If the DNA phosphates form hydrated ion pairs with the cationic groups on the protein (∼4−6 Å charge separation), then carboxylate hydration can dominate the thermodynamics and the reaction is driven by a change in enthalpy. This coupled salt bridge disruption can explain a reduction in the salt concentration dependence of the binding constant. In the case of polyE, the coupled salt bridge disruption hypothesis would predict that as the ionic strength is increased in a solution containing AVP−pVIc·(polyE) complexes, the cationic groups in AVP−pVIc that bind to anionic groups in polyE begin to exchange partners to form salt bridges with carboxylate groups in AVP−pVIc.

There seems as well to be a favorable nonelectrostatic component of the binding interaction between polyE and AVP−pVIc. Upon extrapolation of the line in Figure 5 to 1 M Na^+, correcting for ion pairs yielded a nonelectrostatic free energy of binding, ΔG_0^0, of −6.5 kcal. For comparison, the nonelectrostatic free energy of binding of AVP−pVIc to 12-mer dsDNA is −4.6 kcal (*8*); it is −2.6 kcal for the binding of the gene 32 protein to helical DNA (*19*). These findings imply that a component of the binding free energy under physiological conditions resulted from nonspecific, nonelectrostatic interactions between AVP−pVIc and polyE. However, the dominant factor driving the nonspecific interaction between AVP−pVIc and polyE may be the entropic contribution from the release of counterions.

The observation that polyE can displace DNA from AVP−pVIc (DNA) complexes suggests polymers of glutamic acid could follow the same binding pathway, with the carboxylate side chains of the glutamic acid residues substituting for the phosphates of the DNA in the interaction with cationic residues on AVP−pVIc. A map of the binding of 12-mer ssDNA to AVP−pVIc has recently been obtained by synchrotron X-ray protein−nucleic acid footprinting (*9*) (Figure 6). It shows the DNA spanning the two domains of

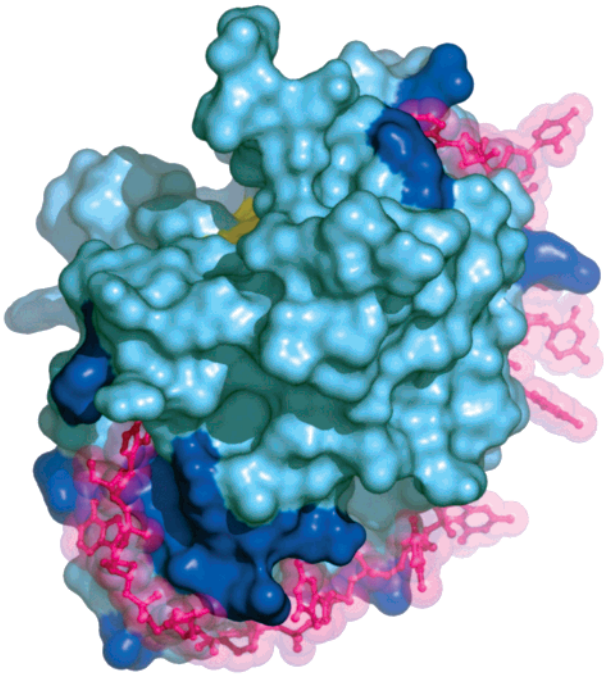

FIGURE 6: Model for the binding of a polyanion to AVP−pVIc. The model is derived from synchrotron X-ray footprinting data (*9*). The AVP−pVIc complex is shown as a cyan-colored molecular surface, with positively charged regions colored blue and the active site residues colored yellow. A potential polyanion binding site is depicted using a 12-mer ssDNA molecule. The DNA is colored red and depicted in ball-and-stick form with a semitransparent surface. The figure was generated using PYMOL (http://pymol.surgeforce.net).

AVP, interacting with the positively charged regions of AVP. The active site of AVP lies in a cleft formed by the interactions of the two domains. Thus, the DNA appears as a strap, holding the two domains of AVP together. More specifically, the model obtained by synchrotron footprinting predicts the DNA wraps around AVP−pVIc, forming a U-turn that exceeds 180°. The cocrystal structure of IHF binding to its specific binding site on dsDNA, the N′ site, shows the DNA wrapped around the protein in a U-turn that also exceeds 180° (*22*). Scanning force microscopy studies (*23*) of the *E. coli* RNA polymerase bound to a promoter show that approximately eight turns of DNA are wrapped around the enzyme in the open complex (*24*−*26*).

Consistent with this interpretation are the large number of cationic amino acid residues in AVP that have anionic amino acid residues nearby. Of the 30 lysine, arginine, and histidine residues in AVP, 70% of them have aspartic acid or glutamic acid residues within 3.5 Å. Of the 12 cationic amino acids within the nine tryptic peptides protected by DNA binding in synchrotron footprinting experiments (*9*), 75% of those cationic amino acid residues are within 3.5 Å of an aspartic acid or a glutamic acid residue. With IHF, all but one of the 23 cationic residues in the DNA binding interface can form salt bridges to carboxylates in free IHF (*21*). The reason only 75% of the cationic amino acid residues can form salt bridges to carboxylates in free AVP−pVIc may be that AVP has several functions other than DNA binding. AVP has an active site for catalysis as well as binding sites for pVIc and actin.

The interaction of AVP−pVIc with polymers of glutamic acid may be a physiologically relevant interaction. Recently, we showed that actin is a cofactor for AVP (*27*). The K_d for the binding of actin to AVP is 4.2 nM (*28*). One AVP binding site on actin is at its C-terminus; of the last eight amino acids of actin, four are identical and three homologous to the last eight amino acids of pVIc. But, there is another binding site on actin for AVP, and this site has all the characteristics exhibited by polyE in its binding to AVP−pVIc (M. T. Brown and W. F. Mangel, unpublished observations). Binding is sensitive to ionic strength, and DNA can completely compete with binding. This site, presumably, is in a region of actin that has a high negative charge density; binding here would restrict AVP activity in the cytoplasm to sites where actin is located.

ACKNOWLEDGMENT

We are grateful to Dr. Tom Record for perceptive discussions about the manuscript, to Dr. Sayan Gupta for Figure 6, and to Vito Graziano for help in the binding analysis.

REFERENCES

1. Weber, J. (1976) Genetic analysis of adenovirus type 2, III. Temperature sensitivity of processing of viral proteins, *J. Virol. 17*, 462−471.
2. Brown, M. T., McGrath, W. J., Toledo, D. L., and Mangel, W. F. (1996) Different modes of inhibition of human adenovirus proteinase, probably a cysteine proteinase, by bovine pancreatic trypsin inhibitor, *FEBS Lett. 388*, 233−237.
3. Hannan, C., Raptis, L. H., Dery, C. V., and Weber, J. (1983) Biological and structural studies with adenovirus type 2 temperature-sensitive mutant defective for uncoating, *Intervirology 19*, 213−223.
4. Mirza, A., and Weber, J. (1980) Infectivity and uncoating of adenovirus cores, *Intervirology 13*, 307−311.
5. Mangel, W. F., McGrath, W. J., Toledo, D. L., and Anderson, C. W. (1993) Viral DNA and a viral peptide can act as cofactors of adenovirus virion proteinase activity, *Nature 361*, 274−275.
6. Webster, A., Hay, R. T., and Kemp, G. (1993) The adenovirus protease is activated by a virus-coded disulphide-linked peptide, *Cell 72*, 97−104.
7. Baniecki, M. L., McGrath, W. J., McWhirter, S. M., Li, C., Toledo, D. L., Pellicena, P., Barnard, D. L., Thorn, K. S., and Mangel, W. F. (2001) Interaction of the human adenovirus proteinase with its 11-amino acid cofactor pVIc, *Biochemistry 40*, 12349−12356.
8. McGrath, W. J., Baniecki, M. L., Li, C., McWhirter, S. M., Brown, M. T., Toledo, D. L., and Mangel, W. F. (2001) Human adenovirus proteinase: DNA binding and stimulation of proteinase activity by DNA, *Biochemistry 40*, 13237−13245.
9. Gupta, S., Mangel, W. F., McGrath, W. J., Perek, J. L., Lee, D. W., Takamoto, K., and Chance, M. R. (2004) DNA binding provides a molecular strap activating the adenovirus proteinase, *Mol. Cell. Proteomics 3.10*, 950−959.
10. McGrath, W. J., Abola, A. P., Toledo, D. L., Brown, M. T., and Mangel, W. F. (1996) Characterization of human adenovirus proteinase activity in disrupted virus particles, *Virology 217*, 131−138.
11. Joshua-Tor, L., Xu, H. E., Johnston, S. A., and Rees, D. C. (1995) Crystal structure of a conserved protease that binds DNA: The bleomycin hydrolase, Gal6, *Science 269*, 945−950.
12. Ding, J., McGrath, W. J., Sweet, R. M., and Mangel, W. F. (1996) Crystal structure of the human adenovirus proteinase with its 11 amino acid cofactor, *EMBO J. 15*, 1778−1783.
13. McGrath, W. J., Ding, J., Sweet, R. M., and Mangel, W. F. (2003) Crystallographic structure at 1.6-Å resolution of the human adenovirus proteinase in a covalent complex with its 11-amino acid peptide cofactor: Insights on a new fold, *Biochim. Biophys. Acta 1648*, 1−11.
14. Mangel, W. F., Toledo, D. L., Brown, M. T., Martin, J. H., and McGrath, W. J. (1996) Characterization of three components of human adenovirus proteinase activity *in vitro*, *J. Biol. Chem. 271*, 536−543.

15. Gill, S. G., and von Hippel, P. H. (1989) Calculation of protein extinction coefficients from amino acid sequence data, *Anal. Biochem. 182*, 319−326.
16. Jensen, D. E., Kelley, R. C., and von Hippel, P. H. (1976) DNA "melting" proteins. II. Effects of bacteriophage T4 gene 32-protein binding on the conformation and stability of nucleic acid structures, *J. Biol. Chem. 251*, 7215−7228.
17. Kuzmic, P., Moss, M. L., Kofron, J. L., and Rich, D. H. (1992) Fluorescence displacement method for the determination of receptor−ligand binding constants, *Anal. Biochem. 205*, 65−69.
18. Spencer, R. D., and Weber, G. (1969) Measurement of subnanosecond fluorescence lifetimes with a cross-correlation phase fluorometer, *Ann. N.Y. Acad. Sci. 158*, 361−376.
19. Record, M. T., Lohman, T. M., and De Haseth, P. (1976) Ion Effects on ligand-nucleic acid interactions, *J. Mol. Biol. 107*, 145−158.
20. Zhang, W., and Nilsson, S. (1993) Helix-coil transition of a titrating polyelectrolyte analyzed with the Poisson−Boltzmann cell model: Effects of pH and counter ion valency, *Macromolecules 26*, 2866−2870.
21. Saecker, R. M., and Record, M. T., Jr. (2002) Protein surface salt bridges and paths for DNA wrapping, *Curr. Opin. Struct. Biol. 12*, 311−319.
22. Rice, P. A., Yang, S., Mizuuchi, K., and Nash, H. A. (1996) Crystal structure of an IHF-DNA complex: A protein-induced DNA U-turn, *Cell 87*, 1295−1306.
23. Dame, R. T., Wyman, C., Wurm, R., Wagner, R., and Goosen, N. (2002) Structural basis for H−NS mediated trapping of RNA polymerase in the open initiation complex at the rmBP1, *J. Biol. Chem. 277*, 2146−2150.
24. Mangel, W. F., and Chamberlin, M. J. (1974) Studies of ribonucleic acid chain initiation by *Escherichia coli* ribonucleic acid polymerase bound to T7 deoxyribonucleic acid. I. An assay for the rate and extent of ribonucleic acid chain initiation, *J. Biol. Chem. 259*, 2995−3001.
25. Mangel, W. F., and Chamberlin, M. J. (1974) Studies of ribonucleic acid chain initiation by *Escherichia coli* ribonucleic acid polymerase bound to T7 deoxyribonucleic acid. II. The effect of alterations in ionic strength on chain initiation and on the conformation of binary complexes, *J. Biol. Chem. 249*, 3002−3006.
26. Mangel, W. F., and Chamberlin, M. J. (1974) Studies of ribonucleic acid chain initiation by *Escherichia coli* ribonucleic acid polymerase bound to T7 deoxyribonucleic acid. III. The effect of temperature on ribonucleic acid chain initiation and on the conformation of binary complexes, *J. Biol. Chem. 249*, 3007−3013.
27. Brown, M. T., McBride, K. M., Baniecki, M. L., Reich, N. C., Marriott, G., and Mangel, W. F. (2002) Actin can act as a cofactor for a viral proteinase, in the cleavage of the cytoskeleton, *J. Biol. Chem. 277*, 46298−46303.
28. Brown, M. T., and Mangel, W. F. (2004) Interaction of actin and its 11-amino acid C-terminal peptide as cofactors with the adenovirus proteinase, *FEBS* Lett. *563*, 213−218.

BI0502240